



NOTCH1 signaling induces pathological vascular permeability in diabetic retinopathy

Khalil Miloudi^{a,b,1}, Malika Oubaha^{c,1}, Catherine Ménard^{c,1}, Agnieszka Dejda^a, Vera Guber^a, Gael Cagnone^{d,e}, Ariel M. Wilson^c, Nicolas Tétreault^a, Gaëlle Mawambo^c, Francois Binet^c, Rony Chidiac^e, Chantal Delisle^e, Manuel Buscarlet^c, Agustin Cerani^c, Sergio Crespo-Garcia^c, Katie Bentley^f, Flavio Rezende^a, Jean-Sebastien Joyal^d, Frédéric A. Mallette^{c,g}, Jean-Philippe Gratton^e, Bruno Larrivée^a, and Przemyslaw Sapieha^{a,b,2}

^aDepartment of Ophthalmology, Maisonneuve-Rosemont Hospital Research Centre, University of Montreal, Montreal, QC H1T 2M4, Canada; ^bDepartment of Neurology-Neurosurgery, McGill University, Montreal, QC H3A 2B4 Canada; ^cDepartment of Biochemistry and Molecular Medicine, Maisonneuve-Rosemont Hospital Research Centre, University of Montreal, Montreal, QC H1T 2M4, Canada; ^dDepartments of Pediatrics, Ophthalmology, and Pharmacology, Centre Hospitalier Universitaire Ste-Justine Research Center, Montréal, QC H1T 2M4, Canada; ^eDepartment of Pharmacology and Physiology, Faculty of Medicine, University of Montreal, Montreal, QC H3C 3J7, Canada; ^fDepartment of Immunology, Genetics and Pathology, Vascular Biology, Uppsala University, 751 85 Uppsala, Sweden; and ^gDepartment of Medicine, Maisonneuve-Rosemont Hospital Research Centre, University of Montreal, Montreal, QC H1T 2M4, Canada

Edited by Janet R. Sparrow, Columbia University, New York, NY, and accepted by Editorial Board Member Carl F. Nathan January 18, 2019 (received for review August 28, 2018)

Diabetic macular edema is a major complication of diabetes resulting in loss of central vision. Although heightened vessel leakiness has been linked to glial and neuronal-derived factors, relatively little is known on the mechanisms by which mature endothelial cells exit from a quiescent state and compromise barrier function. Here we report that endothelial NOTCH1 signaling in mature diabetic retinas contributes to increased vascular permeability. By providing both human and mouse data, we show that NOTCH1 ligands JAGGED1 and DELTA LIKE-4 are up-regulated secondary to hyperglycemia and activate both canonical and rapid noncanonical NOTCH1 pathways that ultimately disrupt endothelial adherens junctions in diabetic retinas by causing dissociation of vascular endothelial-cadherin from β -catenin. We further demonstrate that neutralization of NOTCH1 ligands prevents diabetes-induced retinal edema. Collectively, these results identify a fundamental process in diabetes-mediated vascular permeability and provide translational rationale for targeting the NOTCH pathway (primarily JAGGED1) in conditions characterized by compromised vascular barrier function.

diabetic macular edema | diabetic retinopathy | NOTCH | JAG1 | DLL4

Diabetes mellitus (DM) is a major health challenge of the 21st century (1). One of the most prevalent primary complications of DM is diabetic retinopathy (DR), which is the leading cause of blindness in the working-age population of industrialized countries (2, 3). Initially characterized by nonproliferative DR with early clinical symptoms of microvascular complications such as microaneurysms and retinal hemorrhages, DR can progress to a proliferative form associated with leaky neovessels, vitreal contraction, and retinal detachment. The most common visual complication that compromises central vision in 25% of diabetic patients is diabetic macular edema (DME) (4), a localized thickening and swelling of the macular area secondary to fluid extravasation. While the root causes of pathological permeability of the retinal vasculature have been linked in part to the progressive overproduction of vasomodulatory molecules, such as vascular endothelial growth factor (VEGF) (5, 6), or neuronal factors produced by stressed neurons, such as semaphorins and netrins (7, 8), there remains a void in our understanding of how mature quiescent endothelial cells (ECs) lose junctional integrity.

Extensively described as a critical pathway regulating developmental angiogenesis (7, 9–13), the NOTCH pathway remains active in the adult vasculature (14) and NOTCH signaling has been proposed to influence adult vascular homeostasis (15). Importantly, NOTCH1 has been shown to maintain vascular endothelium (VE) in a quiescent state (16, 17), and aberrations in NOTCH signaling provoke vascular disorders (18–21), in-

cluding pericyte dysfunction (22, 23). In adults, sustained NOTCH1 activity has been observed in atherosclerotic plaques (24), in premetastatic niches (25), and linked to the generation of a proinflammatory senescent-like phenotype in ECs (24, 25).

NOTCH can also signal in a noncanonical manner where uncleaved NOTCH exerts biological function independent of gene transcription (26). Notably, the unprocessed receptor was reported to signal via a complex with β -catenin (27). This later signaling paradigm may be particularly important in the context of cell–cell adhesion but remains to be explored.

Here we report a role for NOTCH1 in maintaining barrier function in healthy retinas and demonstrate that perturbed NOTCH1 signaling in diabetic retinopathy leads to disruption in the blood retinal barrier. We find elevated NOTCH1 ligands JAG1 and DELTA LIKE-4 (DLL4) in both the vitreous of human DME patients as

Significance

Diabetic retinopathy is a major cause of blindness in the working population. The most common cause of visual impairment in diabetic patients is diabetic macular edema (DME). Roughly 40% of patients with DME respond poorly to anti-VEGF therapies, which are a standard of care. Here we provide mechanistic insight for the critical role of NOTCH1 signaling in compromising endothelial junction integrity during diabetes. Besides activating canonical transcriptional pathways, we find that NOTCH1 signaling also provokes disruption of endothelial junctions via noncanonical mechanisms, such as production of nitric oxide and activation of Src signaling, leading to vascular endothelial-cadherin and β -catenin dissociation. Our findings have implications for future therapeutic interventions given that we find elevated NOTCH1 ligands in the vitreous of patients with DME and that their neutralization decreases pathologic vascular permeability.

Author contributions: K.M., M.O., B.L., and P.S. designed research; K.M., M.O., C.M., A.D., V.G., A.M.W., N.T., G.M., F.B., C.D., A.C., S.C.-G., and F.R. performed research; J.-S.J., F.A.M., J.-P.G., B.L., and P.S. contributed new reagents/analytic tools; K.M., M.O., C.M., A.D., G.C., N.T., F.B., R.C., C.D., M.B., A.C., K.B., B.L., and P.S. analyzed data; and K.M., M.O., C.M., B.L., and P.S. wrote the paper.

The authors declare no conflict of interest.

This article is a PNAS Direct Submission. J.R.S. is a guest editor invited by the Editorial Board.

Published under the PNAS license.

¹K.M., M.O., and C.M. contributed equally to this work.

²To whom correspondence should be addressed. Email: Mike.sapieha@umontreal.ca.

This article contains supporting information online at www.pnas.org/lookup/suppl/doi:10.1073/pnas.1814711116/-DCSupplemental.

Published online February 20, 2019.

well as diabetic mouse retinas and by single-cell RNA sequencing (RNA-seq), we provide evidence that within the retina, constituents of the NOTCH1 pathway are primarily expressed in the VE. Besides activating canonical transcriptional pathways, NOTCH1 signaling also provokes disruption of endothelial junctions via noncanonical mechanisms, such as production of nitric oxide and activation of Src signaling, ultimately leading to VE-cadherin and β -catenin dissociation. Neutralizing NOTCH1 ligands decreases pathologic retinal vascular permeability in diabetic retinas.

Results

JAG1 and DLL4 Are Induced in Mouse Diabetic Retinas Secondary to Hyperglycemia. To investigate the kinetics of expression of NOTCH1 and its ligands during progression of DR, we used the streptozotocin (STZ) mouse model of type 1 diabetes mellitus. STZ was administered to 6-wk-old C57BL/6 mice over 5 consecutive days (mice were considered diabetic when their glycemia exceeded 17 mM) (Fig. 1A).

Reverse-transcription qPCR of retinas at 4 and 8 wk of diabetes confirmed that *Jag1*, *Dll4*, and *Notch1* transcripts rose with diabetes (Fig. 1B and *SI Appendix*, Fig. S1). Similarly, retinal protein levels of NOTCH1 ligands JAG1 and DLL4 (Fig. 1C and D) and effector genes *Hes1*, *Hes5*, and *Hey2* were significantly increased at 8 wk of diabetes (Fig. 1E).

Given the presence of NOTCH1 ligands in diabetic retinas, we next investigated if hyperglycemia itself could trigger production of JAG1 and DLL4 directly in ECs. Human microvascular endothelial cells (HRMECs) were exposed to normal culture media with 5 mM glucose, high concentration of D-glucose (25 mM), or nonmetabolized control L-glucose (25 mM). *Jag1* and *Dll4*, as well as *Hes1*, *Hes5*, and *Hey2* transcripts were induced after 24 h of hyperglycemia (25 mM of D-glucose) compared with control normoglycemia or L-glucose (Fig. 1F and G). Similarly, protein expression of JAG1 and DLL4 also rose in HRMECs after 12, 24, or 48 h of hyperglycemia (Fig. 1H), as did secretion of the ligands into supernatant (Fig. 1I). Together, these mouse data provided the rationale to explore the role of the NOTCH1 pathway in diabetes and specifically in diabetes-induced retinal vascular permeability, which is an early feature of the disease (10).

Notch1 Pathway Is Activated in VE During Hyperglycemia and Diabetes. To study the implication of the NOTCH1 pathway in vascular permeability, we first determined the expression of components of this pathway in the retina. Single-cell mRNA transcript analysis of retinas using Drop-seq (28) revealed enrichment in the NOTCH1 pathway in the VE, with certain effectors enriched in Müller glia, astrocytes, and pericytes [Broad Institute MSigDB: Kyoto Encyclopedia of Genes and Genomes (KEGG) Notch signaling pathway] (Fig. 2A and *SI Appendix*, Fig. S2A). A t-distributed stochastic neighbor embedding (t-SNE) plot of different clustered retinal cell types with similar transcriptional profiles (*SI Appendix*, Fig. S2B) revealed high expression of *Notch1* (Fig. 2B), *Notch4* (*SI Appendix*, Fig. S2C), *Jag1*, and *Dll4* (Fig. 2C) in the VE, whereas *Notch2* and *-3* are nonvascular (Fig. 2B and *SI Appendix*, Fig. S2C). *Notch4* was not induced in STZ retinas (*SI Appendix*, Fig. S2D). Immunofluorescence staining confirmed NOTCH1 localization on retinal vessels (*SI Appendix*, Fig. S3A). We next isolated retinal vasculature from diabetic retinas by laser-capture microdissection and quantified transcripts of NOTCH1 ligands. Reverse-transcription qPCR analysis of isolated vessels revealed an increase of *Jag1* and *Dll4* mRNA expression at 8 wk of diabetes compared with citrate-injected controls (Fig. 2D). Expression of both JAG1 and DLL4 was perivascular and on retinal vessels during diabetes as confirmed by immunohistochemistry (*SI Appendix*, Fig. S3B).

Given higher expression of *Notch1* and its ligands in diabetic retinas (Figs. 1E–G and 2D and *SI Appendix*, Fig. S3), and expression of *Notch1* effector genes in the VE of mouse retinas

(Fig. 2E), we investigated the extent of activation of this pathway during diabetes and secondary to hyperglycemic stress. These data confirm that the NOTCH1 pathway is activated in the endothelium of diabetic retinas and likely via hyperglycemia.

JAG1 and DLL4 Compromise Retinal Barrier Function via Dissociation of the VE-Cadherin/ β -Catenin Complex. Given the elevated retinal levels of NOTCH1 ligands in conditions associated with retinal edema, we sought to determine the propensity of either JAG1 or DLL4 to compromise retinal vascular barrier function. We injected 1 μ L of either recombinant JAG1 or DLL4 into the vitreous of adult mice and evaluated vascular leakage. JAG1 was used at a concentration of 2 μ g/mL and similar molar concentration of DLL4 at 1 μ g/mL according to previously established ED50s (29, 30) and vitreal dilution. Both JAG1 and DLL4 increased retinal vascular leakage as visualized in retinal flat-mounts following perfusion with FITC-dextran (Fig. 3A) and quantified by the retinal Evans blue assay for macromolecule extravasation (Fig. 3B and *SI Appendix*, Fig. S4A). Similarly, JAG1 and DLL4 induced vascular leakage in an auricular Miles assay, suggesting a conserved mechanism throughout mature vascular beds (Fig. 3C and D).

VE-cadherin is required for maintaining transendothelial junctions and recruits β -catenin as a stabilizing bridge between cadherins and the cytoskeleton (31, 32). Phosphorylation of VE-cadherin on Y731 leads to dissociation of endothelial adherens junctions and results in loss of barrier function (33, 34). We exposed HRMEC monolayers to JAG1 or DLL4 and immunolocalized phosphorylated VE-cadherin/ β -catenin (35). Both ligands induced phosphorylation of VE-cadherin on Y731 and provoked its internalization (Fig. 3E). These data were confirmed by Western blot analysis of HRMEC lysates that showed phosphorylation of VE-cadherin on Y731 in response to JAG1 or DLL4 (Fig. 3F). We next measured endothelial permeability in vitro by assessing variations in impedance in HRMEC monolayers with electric cell-substrate impedance sensing. Consistent with our in vivo data, stimulation of HRMECs with either JAG1 or DLL4 significantly decreased the impedance of monolayers (JAG1 0.78–3 h; DLL4 0.85–1.25 h, $P < 0.05$) as a result of compromised cell–cell junctions (Fig. 3G). In addition, either JAG1 or DLL4 disrupted junctions at cell–cell contact points as evidenced by confocal immunofluorescence of VE-cadherin and β -catenin (Fig. 3H) and measurement of their colocalization by Pearson coefficient of overlapping voxels (Fig. 3I). Disruption of adherens junction complexes in HRMECs stimulated with either JAG1 or DLL4 was also confirmed by coimmunoprecipitation of VE-cadherin and β -catenin (Fig. 3J). Given the above results where ECs exposed to high glucose increase expression and secretion of JAG1 and DLL4 (Fig. 1I and J), we explored whether VE-cadherin dissociation from β -catenin could be mimicked by hyperglycemia. Similarly to NOTCH1 ligands, exposure to high glucose (25 mM D-glucose) compromised endothelial adherens junctions (*SI Appendix*, Fig. S4B and C) and led to VE-cadherin/ β -catenin dissociation (*SI Appendix*, Fig. S4D). Taken together these data suggest that JAG1 and DLL4 contribute to hyperglycemia-induced vascular permeability.

JAG1 and DLL4 Stimulate VEGFR2–Mediated Src Activation and Nitric Oxide Production. Endothelial barrier function compromise has been extensively studied in the context of VEGFA-induced activation of VEGFR2 (36–38) and consequent tyrosine phosphorylation of Src (35, 39, 40). Given the interplay between VEGF and NOTCH pathways in immature angiogenic vasculature (9, 11, 41), and Drop-seq data revealing high coexpression of *Notch1* and *Vegfr2* in the VE and Müller glia of retina (*SI Appendix*, Fig. S5), we examined the effects of JAG1 and DLL4 on VEGFR-2 and Src activation. Interestingly, either JAG1 or DLL4 can induce VEGFR2 phosphorylation at tyrosine 1175 in

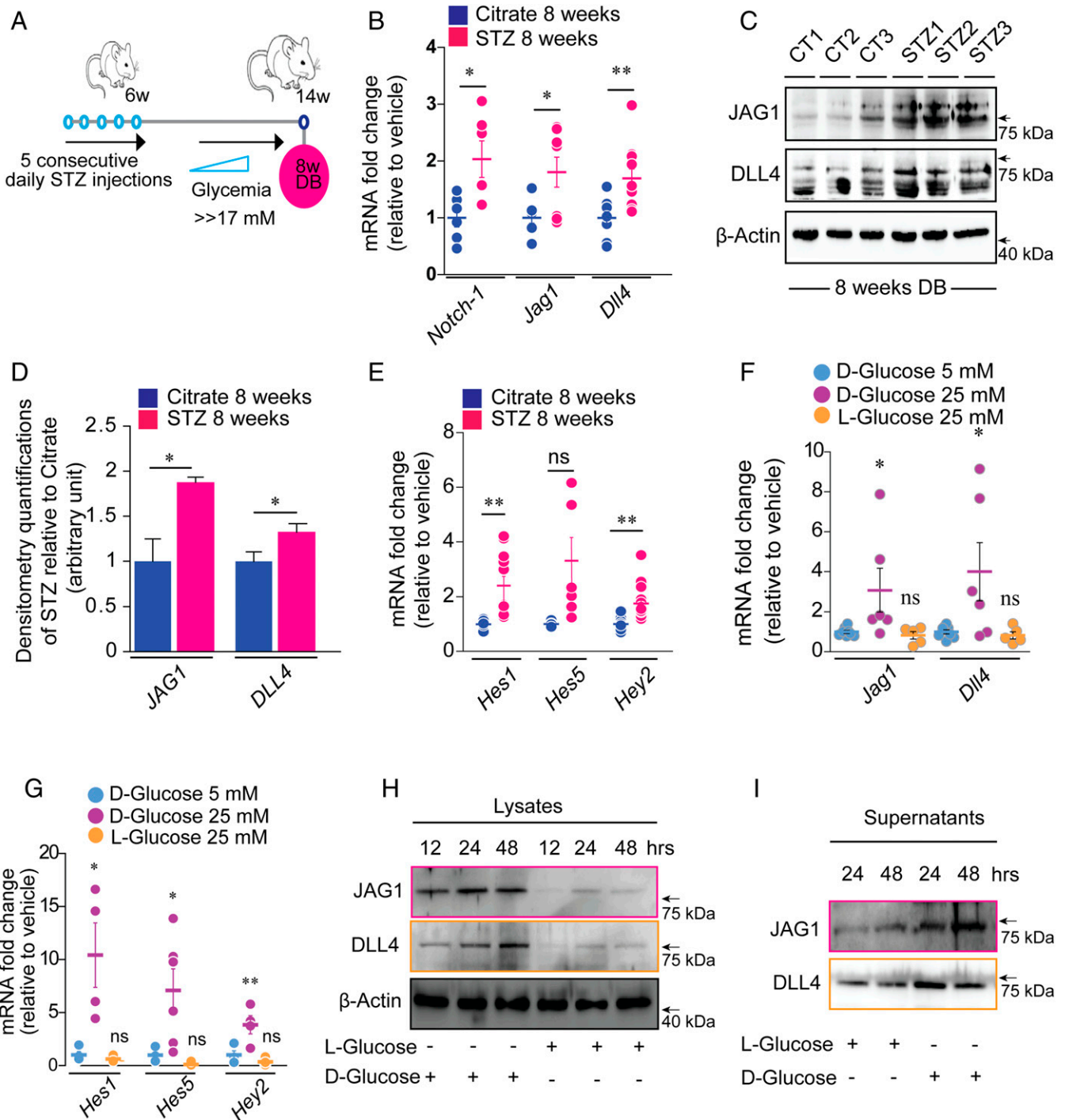


Fig. 1. JAG1 and DLL4 are induced in mouse retinas in diabetes. (A) Scheme explaining STZ administration and blood glucose monitoring of diabetic mice. (B) Real-time qPCR of *Notch-1*, *Jag1*, and *Dll4* transcripts in diabetic retinas at 8 wk of diabetes; *Notch-1* [control (ctl) 1.000 ± 0.1604 , STZ 2.034 ± 0.3224 , $*P = 0.0166$, $n = 6$], *Jag1* (ctl 1.000 ± 0.09357 , STZ 1.805 ± 0.2632 , $*P = 0.0182$, $n = 9$), and *Dll4* (ctl 1.000 ± 0.1093 , STZ 1.694 ± 0.1665 , $**P = 0.0039$, $n = 9-11$). (C) Western blot analysis of retinal whole-cell lysates confirmed that JAG1 and DLL4 were induced at 8 wk of diabetes. (D) Bar graphs for protein densitometry quantifications of JAG1 and DLL4 relative to β -actin. JAG1 (ctl 1.000 ± 0.2482 , STZ 1.879 ± 0.05566 , $*P = 0.0259$, $n = 3$), and DLL4 (ctl 1.000 ± 0.1053 , STZ 1.357 ± 0.06350 , $*P = 0.0439$, $n = 3$). (E) Real-time qPCR for the downstream effectors of Notch1, *Hes1*, *Hes5*, and *Hey2* in diabetic retinas at 8 wk of diabetes; *Hes1* (ctl 1.000 ± 0.04286 , STZ 2.772 ± 0.4950 , $n = 11-13$, $**P = 0.0039$), *Hes5* (ctl 1.000 ± 0.03643 , STZ 3.130 ± 0.8521 , $n = 6$, $P = 0.0547$, NS), and *Hey2* (ctl 1.000 ± 0.04451 , STZ 2.053 ± 0.3192 , $n = 17-19$, $**P = 0.0043$). (F) Real-time qPCR of *Jag1* and *Dll4* transcripts in HRMECs (ctl vs. D-glucose 25 mM vs. L-glucose). *Jag1* (1.000 ± 0.07602 , 3.080 ± 1.093 , 0.8278 ± 0.1874 , $q = 2,537$, $n = 5-8$, $*P < 0.05$), *Dll4* (1.000 ± 0.1078 , 4.004 ± 1.447 , 0.8259 ± 0.1796 , $n = 5-8$, $*P < 0.05$). (G) Real-time qPCR for *Hes1*, *Hes5*, and *Hey2* in HRMECs in varying glycemia (ctl D-glucose 5 mM vs. D-glucose 25 mM vs. L-glucose 25 mM); *Hes1* (1.000 ± 0.3195 , 10.42 ± 3.038 , 0.6187 ± 0.1846 , $n = 3-4$, $*P < 0.05$), *Hes5* (1.000 ± 0.2920 , 7.084 ± 2.046 , 0.1019 ± 0.06145 , $n = 4-6$, $*P < 0.05$), and *Hey2* (1.000 ± 0.3867 , 3.848 ± 0.8546 , 0.3623 ± 0.1381 , $n = 4-6$, $*P < 0.05$). *t* test with Welch's correction (F and G) and (H) Western blot analysis of HRMEC lysates at 12, 24, and 48 h and supernatants from the same cells (I), revealing higher expression of JAG1 and DLL4 under 25 mM D-glucose compared with control L-glucose. ($n = 3$). Data expressed as mean \pm SEM. Statistical analysis: *t* test (B, D, and E), one-way ANOVA with Dunnett's multiple comparison test (F and G).

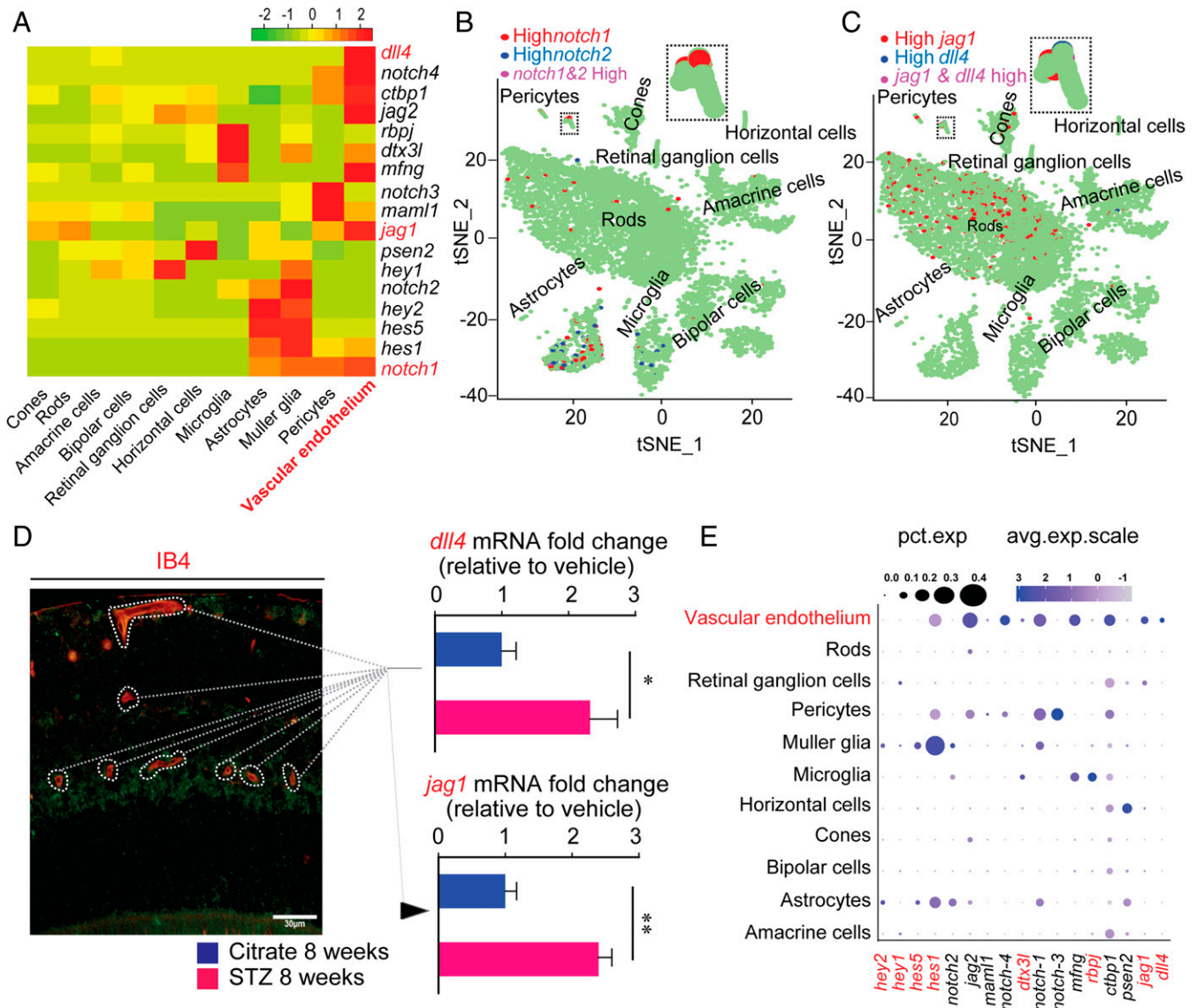


Fig. 2. Notch1 pathway is expressed in retinal VE and activated in diabetes. (A) Heatmap for the Notch1 pathway (KEGG Notch-1 signaling pathway) revealing high expression in the retinal VE, Müller glia, and astrocytes. (B) t-SNE showing that *Notch1* expression is predominantly endothelial compared with *Notch2*. *Jag1* and *Dll4* were also found in the VE (C). (D) Laser-captured microdissection of outlined retinal vessels (red) followed by real-time qPCR confirmed that *Jag1* and *Dll4* are induced at 8 wk of diabetes (*Jag1* Ctl 1.000 ± 0.171 , STZ 2.362 ± 0.2047 $n = 4$, $**P = 0.0022$; *Dll4* Ctl 1.000 ± 0.2164 , STZ 2.322 ± 0.4111 $n = 4$, $*P = 0.0293$). (E) Dot plot representation using Seurat R package, showing highly expressed NOTCH1 and its target genes expressed in retinal endothelial cells. Data expressed as mean \pm SEM. Statistical analysis: *t* test with Welch's correction (D).

HRMECs (albeit considerably less than control VEGFA) (Fig. 4A). We also observed subsequent phosphorylation of its downstream kinase Src at tyrosine 416 (Fig. 4B), which mediates VE-cadherin phosphorylation and internalization at endothelial cell-cell junctions (42, 43).

Another critical mediator of vascular permeability downstream of VEGFR2 is nitric oxide (NO), produced upon activation of endothelial nitric oxide synthase (eNOS) (44). Phosphorylation of Tyr1175 (Fig. 4A) has been coupled to VEGF-induced PI3K activation (44–46). Activation of AKT at serine 473 downstream of VEGFR2/PI3K results in phosphorylation of eNOS on Ser1177 and leads to increased eNOS activation and NO production (47–50). In line, we observed phosphorylation of AKT and eNOS with either JAG1 or DLL4 (Fig. 4C). Importantly, stimulation with either JAG1 or DLL4 leads to production of nitrite (NO_2^- ; the stable breakdown product of NO) with both ligands provoking a ~25% induction of NO

production by endothelial cells (Fig. 4D), as had been previously suggested (51).

To determine if the effects of JAG1 or DLL4 on vascular permeability require noncanonical signaling via VEGFR2, we pretreated HRMECs with Vandetanib [*N*-(4-Bromo-2-fluorophenyl)-6-methoxy-7-((1-methylpiperidin-4-yl) methoxy)quinazolin-4-amine], a small molecule inhibitor of VEGFR2's tyrosine kinase activity (52, 53). Pretreatment of HRMECs with Vandetanib (1 μM) profoundly inhibited JAG1 or DLL4-mediated VEGFR2 phosphorylation (Fig. 4E). Consequently, the endothelial permeability effectors of eNOS (Fig. 4F) and Src/VE-cadherin (Fig. 4E and G) were inhibited. Immunolocalization of the VE-cadherin/ β -catenin complex in confluent HRMECs pretreated with Vandetanib and stimulated with either JAG1- or DLL4-retained tight junctions (characteristic of a quiescent endothelium) compared with cells without Vandetanib (Fig. 4H). Collectively, these data provide evidence that noncanonical NOTCH1 signaling required to loosen endothelial junctions, hinges

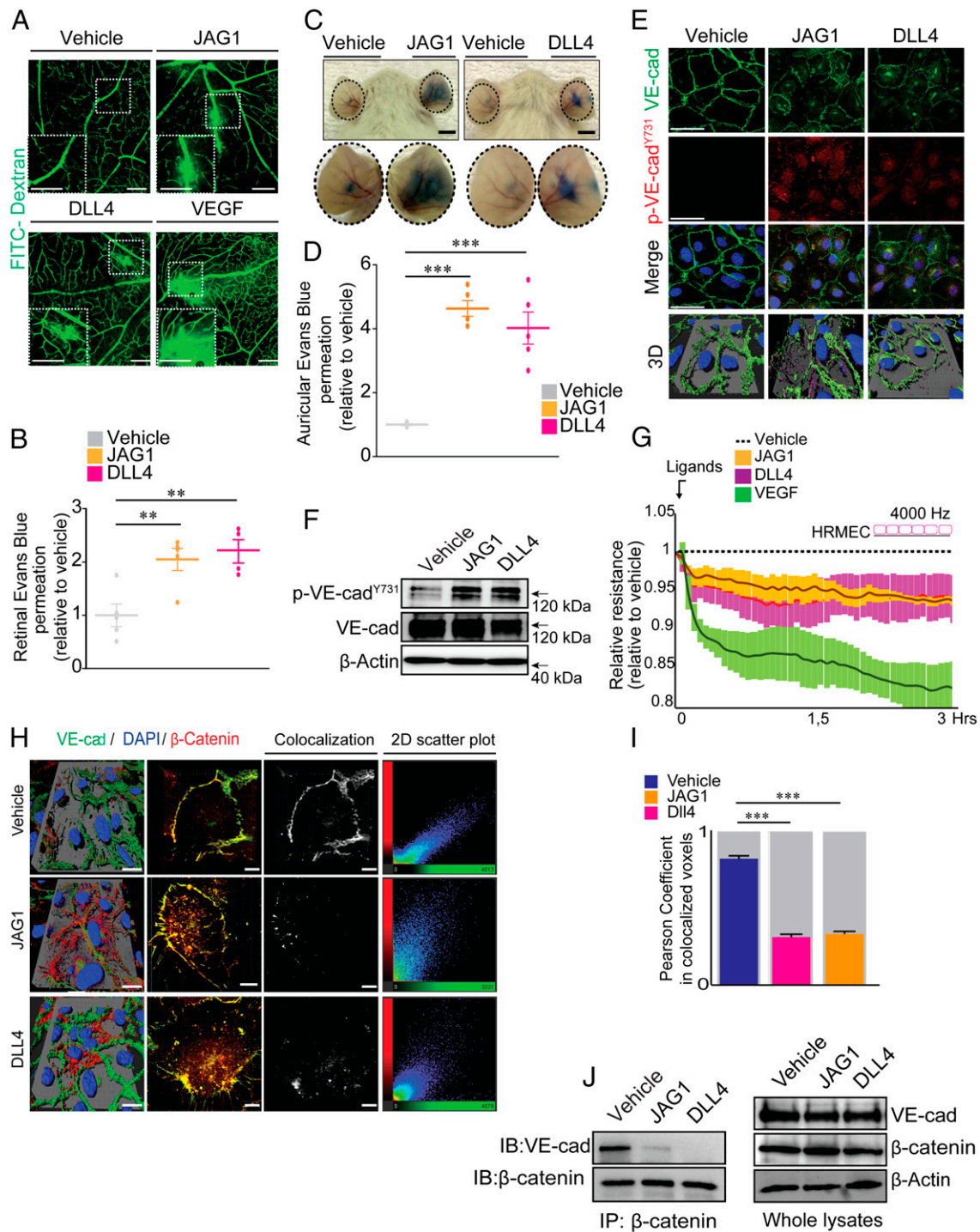


Fig. 3. NOTCH1 ligands induce endothelial permeability and adherens junction dissociation. (A) Retinal flatmounts after vascular permeability assay with FITC dextran following intravitreal injection of vehicle, JAG1, DLL4, or VEGF. Higher magnifications are shown in the *Inset*. (Scale bars, 200 μm .) (B) Quantification of Evans blue extravasation induced by vehicle (PBS), JAG1, or DLL4. JAG1 (1.000 ± 0.2108 , 2.051 ± 0.2064 , $n = 5$, $***P < 0.01$), DLL4 (1.000 ± 0.2108 , 2.201 ± 0.2197 , $n = 4$, $***P < 0.01$). Data presented relative to control. (C) Representative photographs of CD-1 mouse ears in the auricular Miles assay with intradermal injections of vehicle (PBS), recombinant JAG1, recombinant DLL4, or recombinant VEGF and quantification of Evans blue extravasation in D; JAG1 (1.000 ± 0.02879 , 4.635 ± 0.2498 , $n = 4$, $***P < 0.001$) and DLL4 (1.000 ± 0.02879 , 4.021 ± 0.5037 , $n = 5$, $n = 4$, $***P < 0.001$). (Scale bars, 10 μm .) (E) Representative immunofluorescence for VE-cadherin (green), phospho-VE-cadherin^{Y731} (red), and DAPI (blue) in HRMECs stimulated with JAG1 or DLL4 (30 min). Three-dimensional reconstructions of independent experiment. (Scale bars, 30 μm .) (F) Immunoblots for anti-phospho-VE-cadherin^{Y731} in HRMECs stimulated with JAG1 or DLL4. Pan VE-cadherin and β -actin are used as loading controls. (G) Paracellular resistance measured in real time by electric cell-substrate impedance sensing demonstrated that JAG1 (yellow), DLL4 (purple), and the positive control VEGF (green) compromise endothelial barrier function (1–3 h, $n = 3$ –4), compared with vehicle controls (dashed line) ($P < 0.05$ for JAG1 at 0.78–3 h; DLL4 at 0.85–1.25 h). (H) Representative 3D reconstruction of immunofluorescence for β -catenin (red), VE-cadherin (green), and DAPI (blue) in HRMECs stimulated with JAG1 or DLL4 (30 min). (Scale bars, 30 μm .) Colocalization at cell–cell contacts is assessed by 2D scatter plots and (I) Pearson coefficient correlation of measured fluorescence staining of VE-cadherin and β -catenin. $***P < 0.001$. (J) Immunoprecipitation of β -catenin and blotting with for VE-cadherin in HRMECs stimulated with JAG1 or DLL4 show dissociation β -catenin from VE-cadherin. Data expressed as mean \pm SEM. Statistical analysis: one-way ANOVA with Dunnett’s multiple comparison test (B, D, and I).

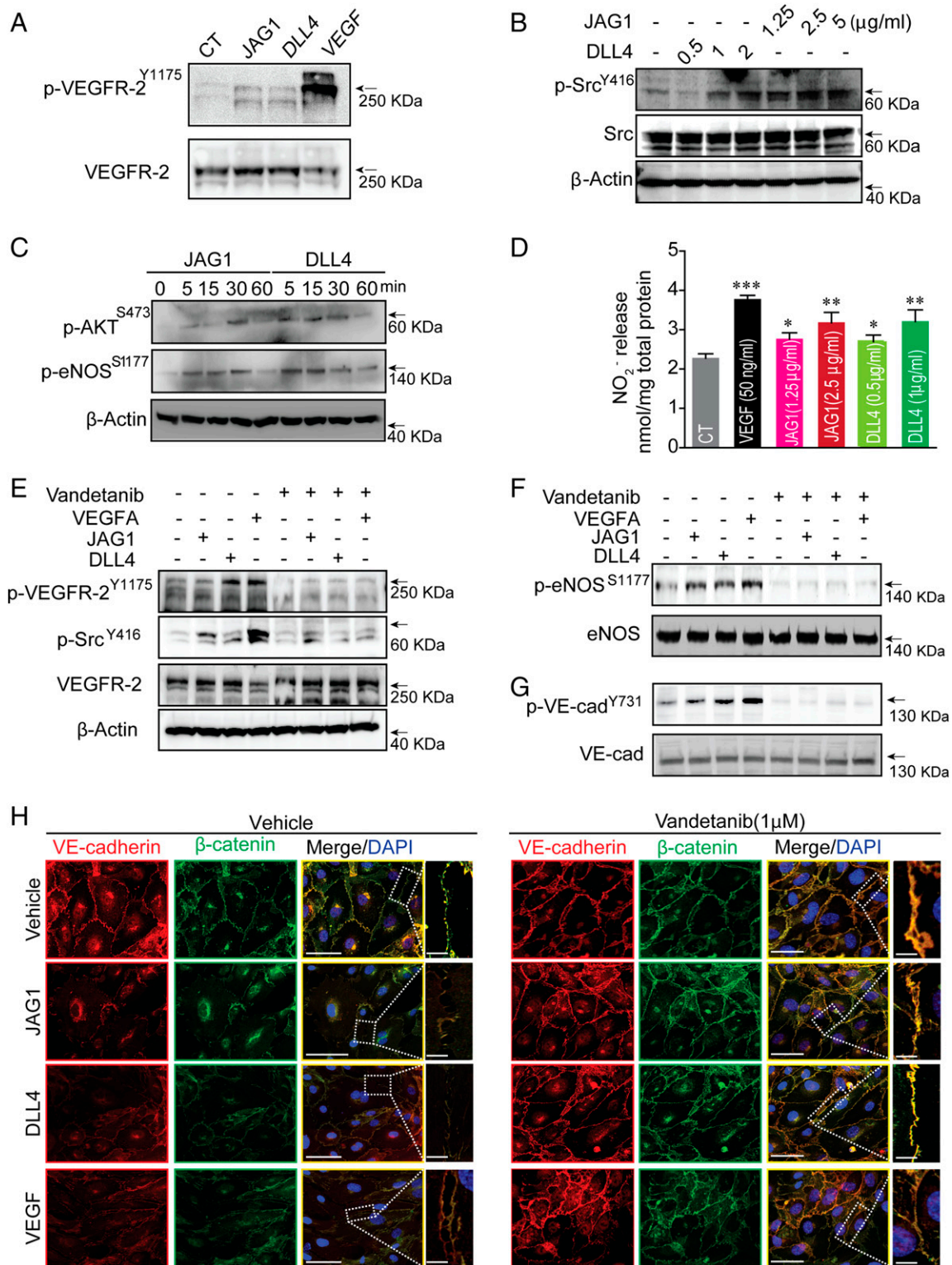


Fig. 4. JAG1 and DLL4 activate VEGFR-2/Src and eNOS/NO pathways. (A) Immunoblot from whole HRMEC lysates stimulated with JAG1 or DLL4 probed for VEGFR-2 phosphorylation at the tyrosines 1175 and total proteins to ensure equal loading. (B) Western blot from HRMEC lysates stimulated for 15 min with ascending doses of JAG1 (1.25, 2.50, 5 μg/ml) and DLL4 (0.5, 1, 2 μg/ml) probed for Src phosphorylation and loading control total Src and β-actin. (C) Immunoblot time course for eNOS and AKT phosphorylation at serines 1177 and 473, respectively, in HRMECs stimulated with JAG1 or DLL4. β-Actin was used as a loading control. (D) Quantification of NO₂⁻ release from serum-starved bovine aortic ECs stimulated for 30 min with different doses of JAG1 (2.50–5 μg/ml), DLL4 (1–2 μg/ml), and VEGF (40 ng/ml). **P* < 0.05, ****P* < 0.01, *****P* < 0.001. (E) Following pretreatment for 24 h with Vandetanib (1 μM), HRMECs were stimulated for 30 min with JAG1 (2 μg/ml), DLL4 (1 μg/ml), or VEGF (40 ng/ml) and p-VEGFR2^{Y1175} and p-Src^{Y416} assessed while (F) phosphorylation of eNOS was determined at serine 1177 and (G) VE-cadherin at tyrosine 731. Pan-VEGFR2, eNOS, VE-cadherin, and β-actin were used as loading controls. (H) Representative confocal micrographs of confluent HRMECs stained for endogenous β-catenin (green), VE-cadherin (red), and DAPI (blue). Higher magnification of outlined regions of cell–cell junctions is shown. (Scale bars: 10 μM; 50 μM in the higher magnification.)

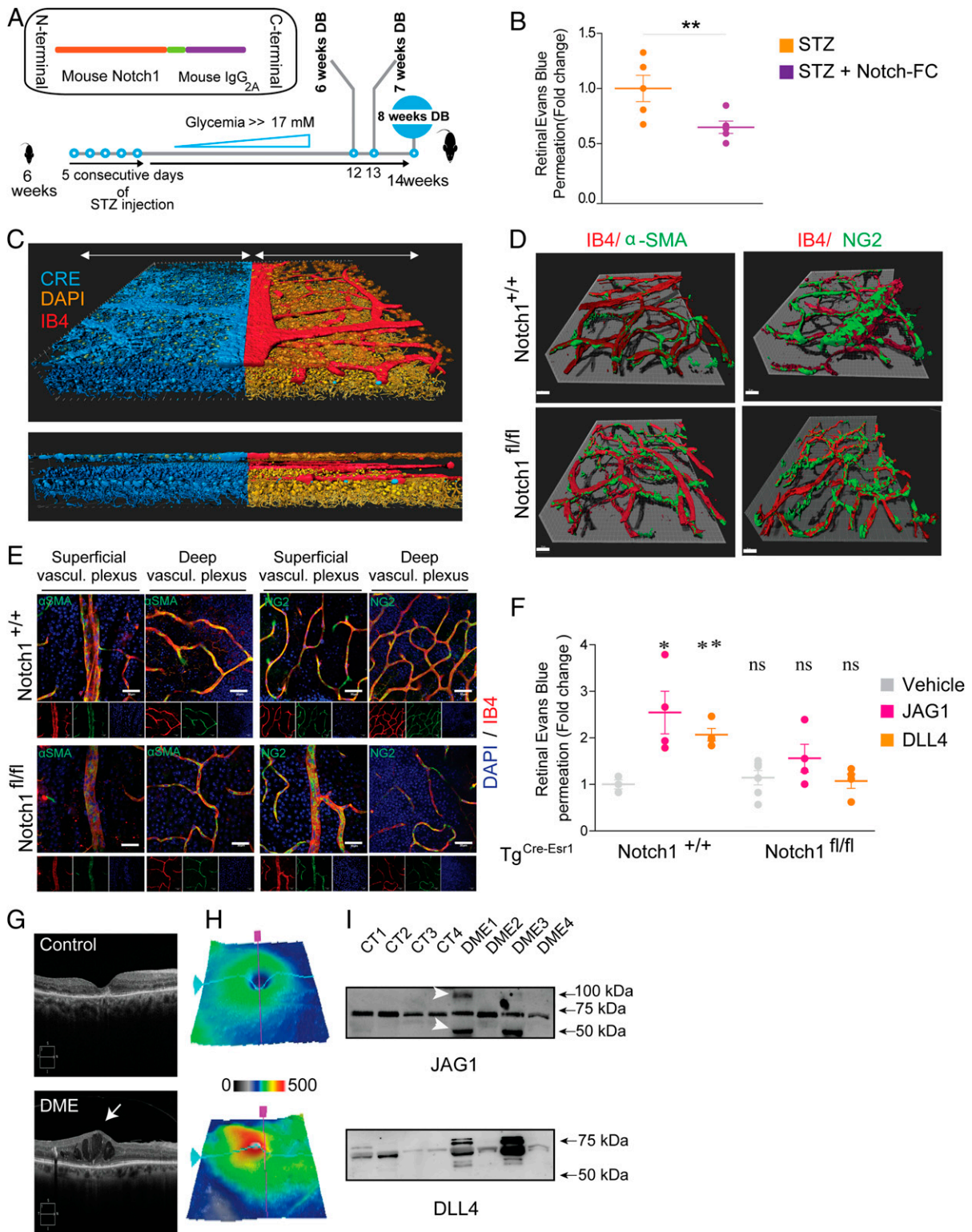


Fig. 5. Inhibition of NOTCH1 and its ligands in vivo reduces pathological vascular permeability. (A) Schematic representation of recombinant NOTCH1-trap that was injected into the vitreous at 6 and 7 wk of diabetes. (B) Quantification of Evans blue extravasation at 8 wk of diabetes indicates reduced vascular permeability with NOTCH1-trap (STZ 1.000 ± 0.1199 , STZ + NOTCH1 Fc 0.6484 ± 0.05632 , $n = 5$, $*P = 0.0291$). (C) Three-dimensional reconstruction confirming vascular expression in $Tg^{Cre-Esr1}/EYFP$ mice. (D) Immunofluorescence of IsolectinB4 (red), α -SMA (green), and NG2 (green) staining in 3D reconstructed retinas, and superficial and deep vascular plexus (E) confirm equal pericytes coverage in $Tg^{Cre-Esr1}/Notch-1^{+/+}$ and $Tg^{Cre-Esr1}/Notch-1^{fl/fl}$ retinas. (Scale bars, 30 μ m.) (F) Quantification of Evans blue dye (red) after intraocular injection of vehicle (PBS), JAG1, DLL4, and VEGF (positive control) in $Tg^{Cre-Esr1}/Notch-1^{+/+}$ and $Tg^{Cre-Esr1}/Notch-1^{fl/fl}$ retinas. $Tg^{Cre-Esr1}/Notch-1^{+/+}$ Veh: 1.000 ± 0.09914 $n = 3$, JAG1: 2.543 ± 0.4574 $n = 4$, $*P < 0.05$, DLL4: 2.067 ± 0.1360 $n = 4$, $*P < 0.05$, $Tg^{Cre-Esr1}/Notch-1^{fl/fl}$ Veh: 1.144 ± 0.1545 $n = 6$, NS, JAG1: 1.561 ± 0.2988 , $n = 4$, NS, DLL4: 1.070 ± 0.1563 $n = 4$, NS. Data expressed as mean \pm SEM. Statistical analysis: t test (B) and one-way ANOVA with Dunnett's multiple comparison test (F). (G) SD-OCT and (H) 3D retinal maps of patients suffering from DME with severe retinal swelling (red) in central foveal zones compared with control patients without retinal vascular pathologies. (I) Western blot of equal volume (10 μ L) of vitreous humor revealed the presence of JAG1 and DLL4 in patients suffering from DME.

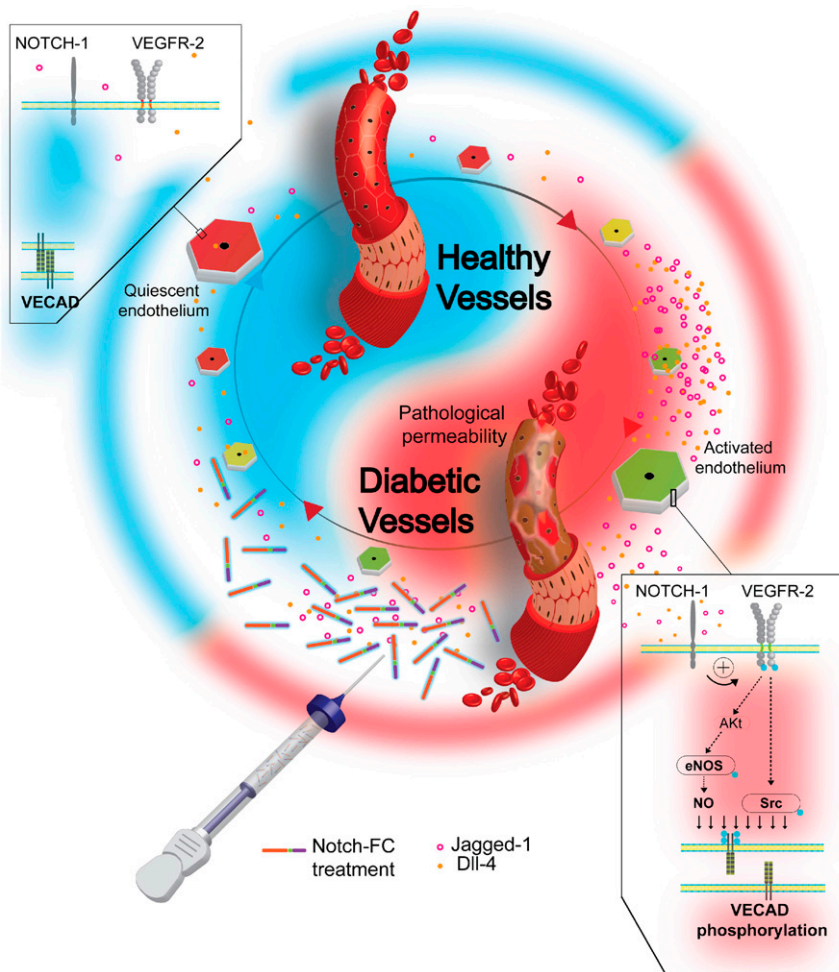


Fig. 6. Graphic representation of findings.

on VEGFR2 and its downstream activation of Src/VE-cadherin and AKT/eNOS/NO pathways.

Inhibition of NOTCH1 Ligands Reduces Pathological Retinal Vascular Permeability. We next investigated the potential therapeutic benefit of blocking ligands of NOTCH1 with a soluble NOTCH1-based trap (Fig. 5A). The soluble NOTCH1-trap neutralizes both JAG1 and DLL4 and prevents them from activating pathways that compromise barrier function, such as VE-cadherin phosphorylation (SI Appendix, Fig. S6A) or dissolution of β -catenin from VE-Cadherin in an HRMEC monolayer (SI Appendix, Fig. S6 B–E). Intravitreal injections of the NOTCH1-trap at 6 and 7 wk after induction of diabetes led to a significant reduction in diabetes-induced vascular permeability by ~30% at 8 wk after STZ-induced diabetes (Fig. 5B).

To verify the requirement of NOTCH1 in JAG1- and DLL4-induced VE permeability, we next generated a whole-animal tamoxifen-inducible (Tam-inducible) Cre mouse ($Tg^{Cre-Esr1}$) to conditionally delete *Notch1*. Given the robust expression of NOTCH1 in endogenous retinal VE (Fig. 2 A, B, and D), we first confirmed that our Tam-inducible Cre recombinase recombines in the retinal vessels. We generated a reporter mouse by breeding $Tg^{Cre-Esr1}$ mice with $B6.129 \times 1-Gt(ROSA)26Sor^{Tm1(EYFP)Cos/J}$ mice and with 3D reconstruction of confocal images, we confirmed Cre expression in retinal vessels (Fig. 5C). $Tg^{Cre-Esr1}$ mice were then crossed with *Notch1^{fl/fl}* mouse to generate a $Tg^{Cre-Esr1}/Notch1^{fl/fl}$ mouse. Tamoxifen was administered intraperitoneally

(at 6–10 wk of age) for 5 consecutive days, which led to an efficient NOTCH1 knockout as determined by immunohistochemistry for retinal vasculature (SI Appendix, Fig. S7A) and in the whole-retinal lysates by Western blot (SI Appendix, Fig. S7 B and C) and qPCR (SI Appendix, Fig. S7D). Importantly, immunofluorescence on retinal flatmounts from $Tg^{Cre/Esr1}/Notch1^{+/+}$ and $Tg^{Cre/Esr1}/Notch1^{fl/fl}$ mice showed a similar levels of coverage for NG2 and α SMA, demonstrating that Tam-inducible NOTCH1 knockout does not affect pericyte or smooth muscle cell coverage of retinal vasculature (Fig. 5 D and E).

We next injected either JAG1 or DLL4 into the vitreous of $Tg^{Cre/Esr1}/Notch1^{+/+}$ and $Tg^{Cre/Esr1}/Notch1^{fl/fl}$ mice and found that mice lacking NOTCH1 maintained baseline vascular permeability, while mice expressing NOTCH1 showed vascular leakage (Fig. 5F). Collectively, these data support the role of JAG1 and DLL4 and their cognate receptor NOTCH1 in diabetes-induced vascular permeability. Additionally, these data suggest that NOTCH1 signaling in diabetes contributes to retinal vascular leakage and that neutralizing NOTCH1 ligands in diabetic retinopathy reduces pathological vascular permeability.

To determine potential clinical significance, we then investigated the levels of NOTCH ligands JAG1 and DLL4 in vitreous of patients suffering from DME (SI Appendix, Table S1), selected according to a macular thickness greater than 250 μ m, as determined by spectral-domain optical coherence tomography (SD-OCT) (Fig. 5G). Representative SD-OCT and 3D retinal maps of

retinas from patients with DME show macular and retinal swelling compared with control patients with nonvascular pathology (Fig. 5 G and H). Western blot analysis of NOTCH1 ligands revealed an increase in isoforms of JAG1 (Fig. 5G, white arrow) and DLL4, in the vitreous of a subset, but not all of patients with DME compared with controls (Fig. 5I and SI Appendix, Fig. S8).

Discussion

While primarily studied in the context of cell specification and vascular development, NOTCH signaling has been considerably less investigated in pathology and its potential roles in driving disease mechanisms remain ill-defined. Here we present evidence that in the retina during diabetes, hyperglycemia stimulates production of JAG1 and DLL4 that through NOTCH1, compromise endothelial junctional integrity by perturbing adherens junctions. While JAG1 and DLL4 are less potent inducers of vascular permeability than VEGFA, they remain relevant in a protracted disease, such as DME, where even subtle triggers of vascular permeability can provide meaningful mechanistic and therapeutic insight (Fig. 6).

NOTCH1 has been suggested to partake in ensuring quiescence of the endothelium and contributing to vascular stability by maintaining proper interaction between pericytes and vascular smooth muscle cells (54). Our data supports that in diabetes and in ECs subjected to hyperglycemic conditions, both canonical and noncanonical NOTCH1 signaling is activated. Similar to our finding, hyperglycemia-induced production of JAG1 by ECs was previously reported in vitro (21). However, the same group demonstrated that knockdown of JAG1 specifically in ECs in vivo can prevent retinal microvasculopathy in diabetic mice (20).

While canonical transcriptional events may influence vascular homeostasis in a chronic manner throughout disease, noncanonical activation of endothelial NOTCH1 provokes rapid destabilization of the VE via mechanisms that lead to phosphorylation of VEGFR2, production of NO, and ultimately result in VE cadherin/ β -catenin complex dissociation. Production of NO via NOTCH activation (particularly via JAG1) has previously been suggested (51) and is particularly relevant given the role of NO in mediating vascular permeability (44, 55, 56). The mechanisms by which NOTCH signaling regulates phosphorylation of VEGFR2 are not well understood. Interestingly, hyperglycemia has been associated with reactive oxygen species (ROS)-dependent phosphorylation of VEGFR2, independently of ligand binding (57). Given that NOTCH increases NO production and has been shown to regulate ROS production in endothelial cells (58), NOTCH1-dependent phosphorylation of VEGFR2 may be a consequence of exacerbated production of ROS in diabetic conditions. Alternatively, VEGFR2 phosphorylation in the presence of NOTCH ligands may result from decreased association of VE-cadherin and VEGFR2, because VE-cadherin has been shown to limit VEGFR2 signaling by preventing its internalization (59).

In concert, these events contribute to diabetes-induced vasogenic edema in the retina and, hence, suggest that the pathway is amenable to therapeutic modulation. Targeting JAG1 and DLL4 is all of the more plausible given that we observe a rise in secreted forms of the proteins and that a NOTCH1-based trap can be employed to neutralize NOTCH1 ligands and attenuate

retinal barrier function breakdown. Therapeutically beneficial modulation of NOTCH signaling with a biologic has been demonstrated for NOTCH3 in cerebral autosomal-dominant arteriopathy with subcortical infarcts and leukoencephalopathy that is characterized by loss of mural cells and vessel instability (60). Machuca-Parra et al. (60) employed a NOTCH3 agonist antibody that activates NOTCH3 and prevented mural cell loss and plasma biomarkers of the disease. While we provide evidence that our NOTCH1-based trap quenches the effects of JAG1 and DLL4 on the VE, we cannot discount direct interaction with plasma membrane-resident effectors.

While typically considered as cell membrane-tethered ligands, we observed that JAG1 and DLL4 are secreted in soluble form during DR and act as paracrine factors. This is similar to what has been described for EC-secreted JAG1 in colorectal cancer, where it promotes cancer stem cells (61), and soluble DLL4, where it prevents choroidal neovascularization in models of age-related macular degeneration (62). Although JAG1 and DLL4 often trigger divergent physiological effects, in our hands both soluble forms seem to compromise retinal barrier function in DR. NOTCH signaling is traditionally activated in response to a polarized signal. Transligands carried by opposing cells activate the NOTCH receptor, whereas *cis*-ligands present on the same cell repress NOTCH activity (63, 64). The disruption of *cis/trans* NOTCH signaling in the presence of excess soluble ligands may favor noncanonical signaling that regulate transcription-independent dissociation of the VE-cadherin/ β -catenin complex and loss of adherens junctions.

Currently, roughly 40% of patients with DME respond poorly to anti-VEGF therapies (65). Moreover, with several anti-VEGF compounds going off patent, there is an interest in elucidating novel druggable therapeutic targets. Overall, our data provide a rationale for targeting the NOTCH1 pathway and its ligands JAG1 and DLL4 for conditions associated with diabetes-induced vascular permeability, such as diabetic macular edema.

Materials and Methods

For detailed methods, please see SI Appendix.

Human Samples. The study conforms to the tenets of the Declaration of Helsinki, and approval of the human clinical protocol was obtained from the Maisonneuve-Rosemont Hospital Ethics Committee (Ref. CER:10059). Patients consented to have their vitreous biopsied before receiving their anti-VEGF treatment and protein content analyzed.

Animals. Studies were performed according to the Association for Research in Vision and Ophthalmology statement for the Use of Animal in Ophthalmic and Vision Research and were approved by the Animal Care Committee of the University of Montreal in agreement with the guidelines established by the Canadian Council on Animal Care.

ACKNOWLEDGMENTS. This work was supported by Canadian Institutes of Health Research Grant 353770 (to P.S.); Heart & Stroke Foundation Canada Grant G-16-00014658 (to P.S.); Foundation Fighting Blindness Canada, the Diabetes Canada Grant DI-3-18-5444 (to P.S.); and Natural Sciences and Engineering Research Council of Canada Grant 418637 (to P.S.). P.S. holds the Wolfe Professorship in Translational Research and a Canada Research Chair in Retinal Cell Biology. C.M. holds a scholarship from the Fonds de Recherche en Santé du Québec.

- World Health Organisation (2015) Global Report on Diabetes. Available at https://apps.who.int/iris/bitstream/handle/10665/204871/9789241565257_eng.pdf;jsessionid=8563331FD5018F74D58858A1960CB8EB?sequence=1. Accessed February 6, 2019.
- Kempner JH, et al.; Eye Diseases Prevalence Research Group (2004) The prevalence of diabetic retinopathy among adults in the United States. *Arch Ophthalmol* 122:552–563.
- Duh EJ, Sun JK, Stitt AW (2017) Diabetic retinopathy: Current understanding, mechanisms, and treatment strategies. *JCI Insight* 2:93751.
- Moss SE, Klein R, Klein BE (1998) The 14-year incidence of visual loss in a diabetic population. *Ophthalmology* 105:998–1003.
- Hammes HP, Feng Y, Pfister F, Brownlee M (2011) Diabetic retinopathy: Targeting vasoregression. *Diabetes* 60:9–16.

- Antonetti DA, Lieth E, Barber AJ, Gardner TW (1999) Molecular mechanisms of vascular permeability in diabetic retinopathy. *Semin Ophthalmol* 14:240–248.
- Cerani A, et al. (2013) Neuron-derived semaphorin 3A is an early inducer of vascular permeability in diabetic retinopathy via neuropilin-1. *Cell Metab* 18:505–518.
- Miloudi K, et al. (2016) Truncated netrin-1 contributes to pathological vascular permeability in diabetic retinopathy. *J Clin Invest* 126:3006–3022.
- Hellström M, et al. (2007) Dll4 signalling through Notch1 regulates formation of tip cells during angiogenesis. *Nature* 445:776–780.
- Benedito R, et al. (2009) The notch ligands Dll4 and Jagged1 have opposing effects on angiogenesis. *Cell* 137:1124–1135.

11. Suchting S, et al. (2007) The Notch ligand Delta-like 4 negatively regulates endothelial tip cell formation and vessel branching. *Proc Natl Acad Sci USA* 104:3225–3230.
12. Dou GR, Wang L, Wang YS, Han H (2012) Notch signaling in ocular vasculature development and diseases. *Mol Med* 18:47–55.
13. Zheng M, Zhang Z, Zhao X, Ding Y, Han H (2010) The Notch signaling pathway in retinal dysplasia and retina vascular homeostasis. *J Genet Genomics* 37:573–582.
14. Hofmann JJ, Iruela-Arispe ML (2007) Notch signaling in blood vessels: Who is talking to whom about what? *Circ Res* 100:1556–1568.
15. Dou GR, et al. (2008) RBP-J, the transcription factor downstream of Notch receptors, is essential for the maintenance of vascular homeostasis in adult mice. *FASEB J* 22:1606–1617.
16. Rostama B, et al. (2015) DLL4/Notch1 and BMP9 interdependent signaling induces human endothelial cell quiescence via P27KIP1 and thrombospondin-1. *Arterioscler Thromb Vasc Biol* 35:2626–2637.
17. Nosedá M, et al. (2004) Notch activation induces endothelial cell cycle arrest and participates in contact inhibition: Role of p21Cip1 repression. *Mol Cell Biol* 24:8813–8822.
18. Rostama B, Peterson SM, Vary CP, Liaw L (2014) Notch signal integration in the vasculature during remodeling. *Vascul Pharmacol* 63:97–104.
19. Gridley T (2010) Notch signaling in the vasculature. *Curr Top Dev Biol* 92:277–309.
20. Yoon CH, et al. (2016) Diabetes-induced Jagged1 overexpression in endothelial cells causes retinal capillary regression in a murine model of diabetes mellitus: Insights into diabetic retinopathy. *Circulation* 134:233–247.
21. Yoon CH, et al. (2014) High glucose-induced jagged 1 in endothelial cells disturbs notch signaling for angiogenesis: A novel mechanism of diabetic vasculopathy. *J Mol Cell Cardiol* 69:52–66.
22. Kofler NM, Cuervo H, Uh MK, Murtomäki A, Kitajewski J (2015) Combined deficiency of Notch1 and Notch3 causes pericyte dysfunction, models CADASIL, and results in arteriovenous malformations. *Sci Rep* 5:16449.
23. Arboleda-Velasquez JF, et al. (2014) Notch signaling functions in retinal pericyte survival. *Invest Ophthalmol Vis Sci* 55:5191–5199.
24. Liu ZJ, et al. (2012) Notch activation induces endothelial cell senescence and pro-inflammatory response: Implication of Notch signaling in atherosclerosis. *Atherosclerosis* 225:296–303.
25. Wieland E, et al. (2017) Endothelial Notch1 activity facilitates metastasis. *Cancer Cell* 31:355–367.
26. Andersen P, Uosaki H, Shenje LT, Kwon C (2012) Non-canonical Notch signaling: Emerging role and mechanism. *Trends Cell Biol* 22:257–265.
27. Kwon C, et al. (2011) Notch post-translationally regulates β -catenin protein in stem and progenitor cells. *Nat Cell Biol* 13:1244–1251.
28. Macosko EZ, et al. (2015) Highly parallel genome-wide expression profiling of individual cells using nanoliter droplets. *Cell* 161:1202–1214.
29. Nobta M, et al. (2005) Critical regulation of bone morphogenetic protein-induced osteoblastic differentiation by Delta1/Jagged1-activated Notch1 signaling. *J Biol Chem* 280:15842–15848.
30. Shimizu K, et al. (1999) Mouse jagged1 physically interacts with notch2 and other notch receptors. Assessment by quantitative methods. *J Biol Chem* 274:32961–32969.
31. Huber AH, Stewart DB, Laurents DV, Nelson WJ, Weis WI (2001) The cadherin cytoplasmic domain is unstructured in the absence of beta-catenin. A possible mechanism for regulating cadherin turnover. *J Biol Chem* 276:12301–12309.
32. Yap AS, Briehner WM, Gumbiner BM (1997) Molecular and functional analysis of cadherin-based adherens junctions. *Annu Rev Cell Dev Biol* 13:119–146.
33. Potter MD, Barbero S, Cheresch DA (2005) Tyrosine phosphorylation of VE-cadherin prevents binding of p120- and beta-catenin and maintains the cellular mesenchymal state. *J Biol Chem* 280:31906–31912.
34. Schlaepfer DD, Hanks SK, Hunter T, van der Geer P (1994) Integrin-mediated signal transduction linked to Ras pathway by GRB2 binding to focal adhesion kinase. *Nature* 372:786–791.
35. Schepcke L, et al. (2008) Retinal vascular permeability suppression by topical application of a novel VEGFR2/Src kinase inhibitor in mice and rabbits. *J Clin Invest* 118:2337–2346.
36. Hudson N, et al. (2014) Differential apical/basal VEGF signaling at vascular blood-neural barriers. *Dev Cell* 30:541–552.
37. Li X, et al. (2016) VEGFR2 pY949 signalling regulates adherens junction integrity and metastatic spread. *Nat Commun* 7:11017.
38. Weis SM, Cheresch DA (2005) Pathophysiological consequences of VEGF-induced vascular permeability. *Nature* 437:497–504.
39. Eliceiri BP, et al. (1999) Selective requirement for Src kinases during VEGF-induced angiogenesis and vascular permeability. *Mol Cell* 4:915–924.
40. Sun Z, et al. (2012) VEGFR2 induces c-Src signaling and vascular permeability in vivo via the adaptor protein TSA. *J Exp Med* 209:1363–1377.
41. Lobov IB, et al. (2007) Delta-like ligand 4 (Dll4) is induced by VEGF as a negative regulator of angiogenic sprouting. *Proc Natl Acad Sci USA* 104:3219–3224.
42. Dejana E, Giampietro C (2012) Vascular endothelial-cadherin and vascular stability. *Curr Opin Hematol* 19:218–223.
43. Lampugnani MG, et al. (2010) CCM1 regulates vascular-lumen organization by inducing endothelial polarity. *J Cell Sci* 123:1073–1080.
44. Fukumura D, et al. (2001) Predominant role of endothelial nitric oxide synthase in vascular endothelial growth factor-induced angiogenesis and vascular permeability. *Proc Natl Acad Sci USA* 98:2604–2609.
45. Dayanir V, Meyer RD, Lashkari K, Rahimi N (2001) Identification of tyrosine residues in vascular endothelial growth factor receptor-2/FLK-1 involved in activation of phosphatidylinositol 3-kinase and cell proliferation. *J Biol Chem* 276:17686–17692.
46. Olsson AK, Dimberg A, Kreuger J, Claesson-Welsh L (2006) VEGF receptor signalling—In control of vascular function. *Nat Rev Mol Cell Biol* 7:359–371.
47. Blanes MG, Oubaha M, Rautureau Y, Gratton JP (2007) Phosphorylation of tyrosine 801 of vascular endothelial growth factor receptor-2 is necessary for Akt-dependent endothelial nitric-oxide synthase activation and nitric oxide release from endothelial cells. *J Biol Chem* 282:10660–10669.
48. Dimmeler S, et al. (1999) Activation of nitric oxide synthase in endothelial cells by Akt-dependent phosphorylation. *Nature* 399:601–605.
49. Oubaha M, Gratton JP (2009) Phosphorylation of endothelial nitric oxide synthase by atypical PKC zeta contributes to angiotensin-1-dependent inhibition of VEGF-induced endothelial permeability in vitro. *Blood* 114:3343–3351.
50. Fulton D, et al. (1999) Regulation of endothelium-derived nitric oxide production by the protein kinase Akt. *Nature* 399:597–601.
51. Chang AC, et al. (2011) Notch initiates the endothelial-to-mesenchymal transition in the atrioventricular canal through autocrine activation of soluble guanylyl cyclase. *Dev Cell* 21:288–300.
52. Wedge SR, et al. (2002) ZD6474 inhibits vascular endothelial growth factor signaling, angiogenesis, and tumor growth following oral administration. *Cancer Res* 62:4645–4655.
53. Hennequin LF, et al. (2002) Novel 4-anilinoquinazolines with C-7 basic side chains: Design and structure activity relationship of a series of potent, orally active, VEGF receptor tyrosine kinase inhibitors. *J Med Chem* 45:1300–1312.
54. Schepcke L, et al. (2012) Notch promotes vascular maturation by inducing integrin-mediated smooth muscle cell adhesion to the endothelial basement membrane. *Blood* 119:2149–2158.
55. Kubes P, Granger DN (1992) Nitric oxide modulates microvascular permeability. *Am J Physiol* 262:H611–H615.
56. Murohara T, et al. (1998) Vascular endothelial growth factor/vascular permeability factor enhances vascular permeability via nitric oxide and prostacyclin. *Circulation* 97:99–107.
57. Warren CM, Ziyad S, Briot A, Der A, Iruela-Arispe ML (2014) A ligand-independent VEGFR2 signaling pathway limits angiogenic responses in diabetes. *Sci Signal* 7:ra1.
58. Vieceli Dalla Sega F, et al. (2017) Context-dependent function of ROS in the vascular endothelium: The role of the Notch pathway and shear stress. *Biofactors* 43:475–485.
59. Lampugnani MG, Orsenigo F, Gagliani MC, Tacchetti C, Dejana E (2006) Vascular endothelial cadherin controls VEGFR-2 internalization and signaling from intracellular compartments. *J Cell Biol* 174:593–604.
60. Machuca-Parra AI, et al. (2017) Therapeutic antibody targeting of Notch3 signaling prevents mural cell loss in CADASIL. *J Exp Med* 214:2271–2282.
61. Lu J, et al. (2013) Endothelial cells promote the colorectal cancer stem cell phenotype through a soluble form of Jagged-1. *Cancer Cell* 23:171–185.
62. Camelo S, et al. (2012) Delta-like 4 inhibits choroidal neovascularization despite opposing effects on vascular endothelium and macrophages. *Angiogenesis* 15:609–622.
63. Bray SJ (2016) Notch signalling in context. *Nat Rev Mol Cell Biol* 17:722–735.
64. Palmer WH, Jia D, Deng WM (2014) Cis-interactions between Notch and its ligands block ligand-independent Notch activity. *eLife* 3.
65. Gonzalez VH, et al. (2016) Early and long-term responses to anti-vascular endothelial growth factor therapy in diabetic macular edema: Analysis of protocol I data. *Am J Ophthalmol* 172:72–79.